Hindawi Publishing Corporation
Mobile Information Systems
Volume 2016, Article ID 3973287, 9 pages
http://dx.doi.org/10.1155/2016/3973287

Research Article

On Novel Access and Scheduling Schemes for IoT Communications

Zheng Jiang, Bin Han, Peng Chen, Fengyi Yang, and Qi Bi

China Telecom Beijing Information Science and Technology Innovation Park, Southern Zone of Future Science and Technology City, Beiqijia Town, Changping District, Beijing 102209, China

Correspondence should be addressed to Zheng Jiang; jiangzh@ctbri.com.cn

Received 17 June 2016; Revised 2 November 2016; Accepted 10 November 2016

Academic Editor: Jose M. Barcelo-Ordinas

The Internet of Things (IoT) is expected to foster the development of 5G wireless networks and requires the efficient support for a large number of simultaneous short message communications. To address these challenges, some existing works utilize new waveform and multiuser superposition transmission schemes to improve the capacity of IoT communication. In this paper, we will investigate the spatial degree of freedom of IoT devices based on their distribution, then extend the multiuser shared access (MUSA) which is one of the typical MUST schemes to spatial domain, and propose two novel schemes, that is, the preconfigured access scheme and the joint spatial and code domain scheduling scheme, to enhance IoT communication. The results indicate that the proposed schemes can reduce the collision rate dramatically during the IoT random access procedure and improve the performance of IoT communication obviously. Based on the simulation results, it is also shown that the proposed scheduling scheme can achieve the similar performance to the corresponding brute-force scheduling but with lower complexity.

1. Introduction

Smart IoT devices are increasingly becoming an integral part of our lives. Such devices are being used in wide areas such as intelligent transportation, health care, environmental monitoring, energy metering, and asset tracking [1]. It is estimated that the number of such devices will grow into billions within few years. While IoT applications are characterized by some unique features which are different with the traditional mobile users, such as huge number of devices, low power consumption, high frequency access of network, massive connectivity, and short message communication, this puts a great pressure for the existing LTE networks. For tackling the new IoT requirement and improve the network efficiency for IoT communication, the related standardization work has been carried out in 3GPP, such as the Rel-13 LTE MTC (machine type communication), where its feature enables a 1.4 MHz compatible carrier which could be overlaid within 20 MHz LTE signal without interference [2], and the Rel-14 NB-IoT (Narrow-Band Internet of Things), which is further improving the LTE IoT support and will provide support of a massive number of low-throughput devices, low delay sensitivity, ultralow device cost, low device power consumption, and optimized network architecture [3]. The NB-IoT can be deployed in-band, utilizing resource blocks within a normal LTE carrier, or in the unused resource blocks within an LTE carrier's guard-band, or stand alone for deployments in a dedicated spectrum.

Even with the new support from LTE-A MTC and NB-IoT, the varied service requirements of IoT are not satisfied sufficiently because the new features introduced by either MTC or NB-LOT have to consider a certain degree of backward compatibility with current LTE system, therefore sacrificing the flexibility of system design and new technical introduction. So all professionals agree that the scenario and requirement of IoT will still be one of the key research areas in the next generation system design and these rapidly increased requirements are expected to be satisfied finally in the 5th generation (5G) wireless communications [4, 5], for example, higher spectral efficiency, massive connectivity, and lower latency.

One of main challenges of IoT communication is massive connectivity and short message communication: for example, such devices are most of the time inactive but regularly access

the network for minor/incremental report updates with no human interaction. To address this challenge, a few schemes have been proposed recently. A new waveform scheme based on biorthogonal frequency division multiplexing was proposed to allow unused frequencies such as guard bands to transmit IoT data [6]. Some multiuser superposition transmission (MUST) schemes have been recently actively investigated [7–11]; MUST can improve spectral efficiency and accommodate much more IoT devices by introducing the controllable interferences to realize overloading with the cost of slightly increased receiver complexity. In [12], a novel scheduling scheme was proposed to reduce the collision rate for IoT access. It can be observed that all of these above works aim to improve the connectivity and communication capability for 5G IoT communication by varied approaches, such as new waveform, new spreading code, and scheduling scheme.

On the other hand, it is well known that massive MIMO is one of the core technologies expected to be adopted by 5G systems. With massive MIMO, one sector can serve tens of user equipment (UEs) simultaneously on the same time-frequency resource; therefore, many schemes were proposed to maximize utilization of the spatial degree of freedom (DOF) introduced by massive MIMO to improve the cellular system performance [13–16]. However until now, utilizing this additional spatial degree of freedom to enhance the IoT communication is not investigated deeply. Moreover, for IoT devices, their distribution, and traffic type are different with traditional mobile UEs, such as their semistatic spatial distribution, short message transmission, and dense communication requests within the short span of time. Therefore, the spatial DOF utilization and resource scheduling for IoT devices have unique features and shall be well exploited.

In this paper, the spatial grouping of IoT devices based on their distribution is investigated, and the novel preconfigured access scheme is proposed to reduce the collision rate of random access; furthermore, the joint spatial and code domain scheduling scheme is proposed to improve the performance of IoT communications. The performance of the proposed scheme is illustrated by simulations and compared with the random scheduling scheme. The results show that the proposed scheme outperforms the random scheduling with and without MUSA because of the additional spatial-domain multiplexing gain. It is also shown in our simulations that the proposed scheduling scheme can exhibit the close performance to the brute-force scheme with lower computational complexity.

In this paper, in order to clarify the IoT device and conventional mobile subscriber, the word "users" refers to IoT devices and word "UEs" refers to conventional mobile subscribers.

The remainder of this paper is organized as follows: Section 2 describes the system model and the features of IoT scheduling utilized to introduce the novel access and spatial-domain scheduling scheme. Section 3 discusses the proposed access and scheduling scheme based on user spatial grouping. Furthermore, the performance and computational complexity of the proposed scheme are analyzed. In Section 4, the simulation results are provided. Finally, Section 5 concludes the paper.

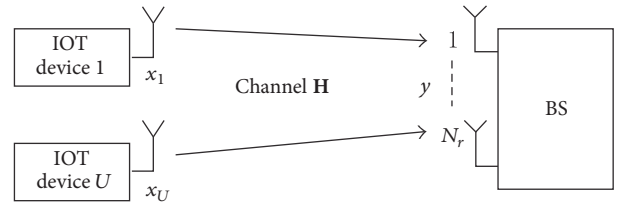

Figure 1: A massive MIMO BS to serve IoT devices.

2. System Model and Feature of IoT Scheduling

2.1. System Model. In this section, the uplink massive MIMO system is given, as shown in Figure 1; as most of IoT devices are the monitors and sensors, they gather information from the monitoring equipment and environment and then report to control center.

The base station (BS) is equipped with N_r antennas to receive the messages from U IoT devices with one antenna.

We assume that $\mathbf{H}_n = [\mathbf{h}_{1,n}, \ldots, \mathbf{h}_{n_r,n}, \ldots, \mathbf{h}_{N_r,n}]^T$ is the frequency channel matrix of size $N_r \times U$ that represents the channel between the BS and U IoT devices on the nth subcarrier.

$\mathbf{h}_{n_r,n} = [h_{1,n_r,n}, \ldots, h_{u,n_r,n}, \ldots, h_{U,n_r,n}]$, $h_{u,n_r,n}$ is the channel statistic information of device u on the nth subcarrier in n_rth antenna.

The received signal of BS is denoted as

$$\mathbf{y}_n = \mathbf{H}_n \mathbf{x}_n + \mathbf{n}_n, \tag{1}$$

where $\mathbf{y}_n$ denotes the collection of received symbols from all the U IoT devices on the nth subcarrier and $\mathbf{x}_n$ is the transmitted signal vector of dimensions $U \times 1$, $\mathbf{x}_n = [x_{1,n}, x_{u,n}, \ldots, x_{U,n}]^T$, where x_u is the transmitted symbol for user u on the nth subcarrier. $\mathbf{n}_n$ denotes additive complex Gaussian noise with zero mean and variance σ_0^2.

Based on the system model described in (1), the MMSE frequency-domain equalization is performed to mitigate the user interference, where the MMSE matrix can be expressed as

$$\mathbf{w}_{\mathrm{MMSE}} = \left(\mathbf{H}_n^H \mathbf{H}_n + \sigma^2 \mathbf{I}\right)^{-1} \mathbf{H}_n^H. \tag{2}$$

The estimated symbol $\hat{\mathbf{x}}_n$ after MMSE frequency-domain equalization (FDE) is

$$\hat{\mathbf{x}}_n = \mathbf{w}_{\mathrm{MMSE}} \mathbf{y}_n. \tag{3}$$

For uplink, BS can achieve channel statistic information (CSI) $\mathbf{H}_n$ of all users by using the uplink pilot send by UEs; then SINR for each user can be calculated by

$$\mathrm{SINR}_{u,n} = \frac{\left|\mathbf{h}_{u,n}\right|^2}{\sigma_0^2 + \sum_{u \neq u'} \left|\mathbf{h}_{u',n}\right|^2}, \tag{4}$$

where $\mathbf{h}_{u,n} = [h_{u,1,n}, \ldots, h_{u,N_r,n}]^T$ is the channel statistic information of N_r antennas of uth user on the nth subcarrier and the $\mathrm{SINR}_{u,n}$ is the SINR of uth user on nth subcarrier. Based on $\mathrm{SINR}_{u,n}$, BS can schedule the proper UEs to transmit their information in uplink.

2.2. Feature of IoT Scheduling. For conventional cellular system, the main target of the scheduling scheme is maximizing the cell throughput and spectral efficiency on the basis of maintaining user fairness to fulfill user growth traffic requirement; therefore, based on this scheduling target, the cost function can be mathematically described by

$$\left(S'_U, S'_N\right) = \arg\max \sum_{u\in S_U, n\in S_N} \log_2\left(1 + \mathrm{SINR}_{u,n}\right), \quad (5)$$

where S_U, S_N are the sets of all user and subcarrier indexes and S'_U, S'_N are the sets of indexes corresponding to the scheduling users and their operating subchannels, respectively. However, considering some unique features of IoT application, as mentioned before, the target of scheduling scheme for IoT communication is different from the conventional mobile system and shall be to maximize the number of active IoT devices to fulfill their dense communication requests within short span of time.

Therefore, we define a utility function that

$$\mathrm{sgn}(x) = \begin{cases} 1, & x \geq 0, \\ 0, & \text{otherwise}, \end{cases} \quad (6)$$

and the cost function of the number of active user maximization can be described by

$$\left(S'_U, S'_N\right) = \arg\max \sum_{u\in S_U, n\in S_N} \mathrm{sgn}\left(\mathrm{SINR}_{u,n} - V_{\mathrm{SINR}}\right), \quad (7)$$

where V_{SINR} is the predetermined threshold of SINR which shall be the minimum value of SINR to maintain the normal operation of IoT devices and V_{SINR} is assumed to be equal for all IoT devices in this paper.

In order to maximize the number of the active IoT devices and system spectral efficiency, some multiuser superposition transmission (MUST) schemes have been proposed recently [7–11]; MUST introduces some controllable interferences to realize overloading at the cost of slightly increased receiver complexity. As a result, higher spectral efficiency and more connectivity can be achieved. However, the existing scheduling schemes of MUST mainly force on the power-domain or code domain to schedule users to multiplex the same time-frequency resources and not exploit the spatial degree of freedom (DOF) based on the user distribution to accommodate more user access and improve the system spectrum efficiency, especially for IoT communication.

Multiuser shared access (MUSA) is one of the typical MUST schemes recently proposed. In the uplink MUSA system, symbols of each user are spread by a spreading sequence which is picked randomly from a sequence pool by access user. Then all spreading symbols are transmitted over the same time-frequency resources [21, 22]. At the receiver, SIC is performed to separate superimposed symbols according to the SINR difference. The typical overloading factor of MUSA is 150%.

Actually if the spreading sequences of MUSA in the resource pool can be reused by the different IoT devices based on their spatial distribution and proper scheduling, then the access number and performance capacity can be improved dramatically. Hence, the user spatial DOF shall be introduced in the scheduling scheme of MUSA to accommodate more user access and improve system capacity for 5G IoT communication.

If we research the distribution and location of IoT devices, we will find that different types of IoT devices may have the different spatial distribution. For example, as shown in Figure 2, there are three types of IoT devices: one is the sensors around the parking spots; the location height of this type of sensors is below 2 m; the second type of IoT devices is the traffic monitor located on the street pole; the height of them is about 6–8 m; the third type is the wireless surveillance cameras or environment detectors installed in the shopping mall or high rise building; the height of this type is a uniform distribution on the vertical height from about 3 m to the top of the building. So it can be observed that the different usage types of IoT devices may be in different spatial locations; meanwhile, once the IoT devices are installed, their positions are not changed frequently, not like conventional mobile users. Based on their static spatial characteristic, IoT devices can be separated into different spatial groups previously, and the devices in different spatial groups can share the same set of spreading sequences for random access and data transmission. Therefore, with multiplexing the spreading sequences, the overloading factor of systems can be increased obviously.

Meanwhile, because of the lack of site, the eMBB and eMTC services may be deployed in the same site in most cases; this condition is similar to the current 4G condition. Utilizing the advantage of eMBB and eMTC colocated deployment, we can use massive MIMO which is used for eMBB originally to enhance the eMTC performance conveniently. Hence, we can use the spatial DOF to increase the number of active IoT devices in 5G massive MIMO system.

Although BS can schedule uplink multiuser transmission based on channel estimation by brute-force scheduling scheme, with the explosion of communication request from IoT devices, the complexity of the brute-force scheduling will increase considerably and become unacceptable.

Hence, in the next section, the preconfigured access scheme and the joint spatial and code domain scheduling scheme with lower complexity are proposed to improve the system performance based on user spatial grouping.

3. On Novel Access and Scheduling Schemes

In the proposed schemes, the strategy is designed in the following three parts:

(1) Based on user (IoT device) location and their channel measurement, BS can split whole channel space into several disjoint subspaces by using prebeamforming matrix and then partition its serving user into several subspace groups with approximately similar channel covariance eigenvectors.

(2) Based on the spatial grouping of users, the preamble code can be reused by users in different spatial group during the random access procedure.

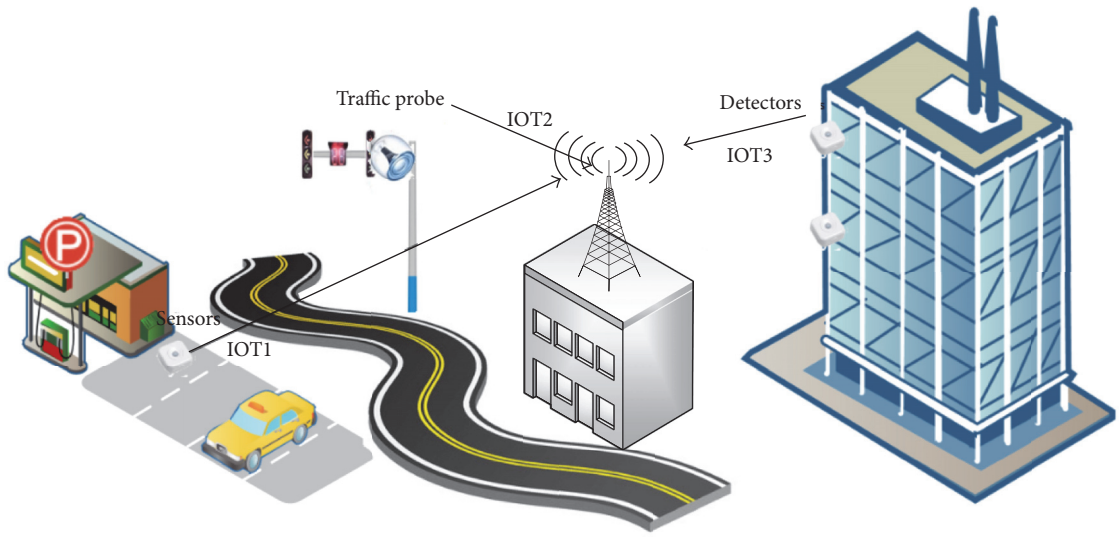

Figure 2: The spatial distribution of varied IoT devices.

(3) For IoT scheduling, the spatial and code domain characters of each user can be identified by a set of indices, that is, {spatial group index g, spreading sequence index m}. For users marked with different spreading sequence indices or users marked with same spreading sequence index and different spatial group indices, they can be scheduled on the same time-frequency resource.

Among the above, the user spatial grouping, preamble multiplexing, and user scheduling in spatial and code domain are three key issues for the system performance; the following discussion will focus more on the strategies of these three issues.

3.1. User Grouping. As mentioned before, in order to exploit effectively the access and joint scheduling approach, the users will be partitioned into spatial groups according to the following qualitative principles: (1) users in the same group have channel covariance eigenspace spanning approximately a given common subspace, which characterizes the spatial group; BS can get this information by UE CSI estimated based on uplink pilots; (2) the subspaces of different spatial groups which served on the same time-frequency resource by joint scheduling must be approximately mutually orthogonal or at least have empty intersection.

In this paper, the fixed quantization algorithm of user grouping is employed; it is considered as an effective and low complexity scheme for the implementation in practical network.

In fixed quantization algorithm, based on the geometry of the user locations and their channel scattering, U users can be divided into G subspace groups, and the subspace of gth group is $\mathbf{V}_g \in \mathbf{R}^{N_r \times r_g}$, $g \in \{1, 2, \ldots, G\}$. As the locations of most IoT devices are almost fixed, the subspace $\mathbf{V}_g$ can be predetermined based on the CSI of IoT devices and fulfill the maximal d_{V_g}, $g \in \{1, 2, \ldots, G\}$. d_{V_g} is

$$d_{V_g} = \min\left\{d_c\left(\mathbf{V}_g, \mathbf{V}_{g'}\right)\right\}$$
$$d_c\left(\mathbf{V}_g, \mathbf{V}_{g'}\right) = \left\|\mathbf{V}_g\mathbf{V}_g^H - V_{g'}V_{g'}^H\right\|_F^2, \tag{8}$$

where d_c is the chordal distance of two matrices, G is the number of spatial groups, r_g is the number of dominant eigenvalues of channel covariance $\mathbf{R}_g$, $\mathbf{V}_g$ is the dominant eigenvectors of R_g with respect to r_g, and $\mathbf{R}_g$ is the channel covariance matrix of users in gth subspace group.

It is easy to see that if $\sum_{g=1}^{G} r_g = N_r$, then we can choose $\{\mathbf{V}_g\}$ as disjoint subsets of the columns of a unitary matrix of dimensions $N_r \times N_r$, such that all group subspaces are mutually orthogonal and d_{V_g} is maximized. Here the disjoint blocks of adjacent columns of the unitary DFT matrix can be used as group subspaces.

For example, if we suppose $G = 3$ and assign $r_g = \lfloor N_r/G \rfloor = r$, and let $\mathbf{F}$ denote the unitary DFT matrix, then, we have $\mathbf{V}_g$ formed by taking the $(g-1)\times r+1$ to $g\times r$ columns of matrix $\mathbf{F}$ [23].

Once $\mathbf{V}_g$ is predetermined, based on the set of user channel information $\mathbf{h}_{u,n}$, $u = 1, 2, \ldots, U$, the users can be partitioned into different spatial groups.

For user grouping, there is a threshold α and let $d_c^* = d_c(\mathbf{V}_g, \mathbf{V}_{g'})$, $d_{g,u} = d_c(\mathbf{V}_g, \mathbf{h}_{u,n})$; if this user's $d_{g,u} < \alpha d_c^*$, we assume that the uth user only belongs to spatial group g and if $\alpha d_c^* < d_{g,u} < d_c^*$ and $\alpha d_c^* < d_{g',u} < d_c^*$, this means that uth user is located in the intersection of $\mathbf{V}_g$ and $\mathbf{V}_{g'}$ subspaces; hence, user u can be assigned to both gth and g'th spatial groups. Based on the user grouping, two sets S_u and S_g can be obtained, S_u is a set of the spatial group indexes $g \in (1, G)$ that the uth user belongs to, and S_g is a set of the user indexes $u \in (1, U)$ that the gth spatial group contains.

In this algorithm, the group subspaces are fixed a priori based on the geometry of users and their CSI. When we increase the number of fixed quantization subspaces to reduce coverage holes, the overlapping between different spatial groups will also increase and cause the strong interferences of intergroups. In this case, we allocate different orthogonal spreading sequences dynamically for users who belong to adjacent groups in order to reduce the interference of intergroups, and the dynamic allocation scheme of the spreading sequences will be given in the proposed joint scheduling scheme in Section 3.3.

As the location of IoT devices is fixed, their channel characteristic is more static than the traditional mobile UEs; therefore, the spatial grouping for IoT devices is more easily performed.

3.2. Preconfigured Scheme for Random Access. Random access is generally performed when the IoT devices turn on and send their reports to control center. In the random access procedure, a user sends a random access preamble to BS by choosing it randomly from a preamble pool which is preallocated by BS. Once the different users send the same preamble, the collision of random access will happen.

In our scheme, based on the spatial orthogonal user grouping, the preamble codes can be shared in the different spatial groups; therefore, more IoT devices can initiate a random access procedure to transmit the uplink message.

However, as the users located in the overlapping areas of different spatial groups can cause the random access collision with the users in adjacent spatial groups if they select the same preamble code, the preconfigured scheme is proposed to reduce the collision rate of these users by preconfiguring preamble pools of spatial groups for these users selection in their random access procedure.

The proposed preconfigured scheme is suggested to schedule the users to start from the user who has the largest number of spatial groups that this user belongs to, because this user has the most spatial group resource available for preconfiguration.

In this sense, assuming that user u_0 has the largest number of spatial groups that it belongs to, therefore the set S_{u0} can be obtained, and in addition we have the set $U_{g_0} = \{g, g \in S_{u0}\}$.

The g^*th spatial group, of which the preamble pools can be used for the u_0th user, can be selected by [24]

$$g^* = \arg\max_{g \in U_{g_0}} \left(N_g^*\right), \tag{9}$$

$$N_g^* = \min_{u \in S_g,\, g \in U_{g_0}} \left(\text{size}\left(S_u\right)\right), \tag{10}$$

where size(S_u) is the utility function to measure the size of the set S_u. The above process follows the principle of leaving the maximal spatial groups for the next loop to perform the preamble pool preconfiguration.

The preconfigured scheme for random access can be described as follows:

(I) Partition users into predetermined G spatial groups based on their CSI.

(II) Preconfigure the preamble resources which are used for user random access. Note that we can share the same preamble resources for users in different spatial groups.

(III) For the users belong to several spatial groups, they can select the preamble resources with one of these groups which is selected based on (9) in their random access procedure.

3.3. Joint Scheduling in Spatial and Code Domain. In this section, we discuss the scheduling scheme for IoT communication. Based on user spatial grouping and their initially estimated SINR, the joint spatial-code scheduling scheme is proposed to maximize the number of active users. Compared with brute-force search scheme with exponential complexity [24], the proposed scheme has less complexity and close performance.

In proposed scheme, a scheduling matrix $\mathbf{M}_S$ with the size of $G \times UN_c$ is defined. The row wise of $\mathbf{M}_S$ stands for the spatial group indexes, and the column wise of $\mathbf{M}_S$ stands for the user index and subcarrier index which the user requests. G is the number of spatial groups; U and N_c are the number of users and subcarriers, respectively. If the uth user and his request nth subcarrier in the gth group have not been scheduled, the $(g, (u-1)N_c + n)$ entry of $\mathbf{M}_S$ denoted by $m_{g,u,n}$ is set to "1" (or otherwise "0"). And we define a resource matrix $\mathbf{M}_C$ with the size of $G \times CN_c$, the row wise of $\mathbf{M}_C$ stands for the group indexes, and the column wise of $\mathbf{M}_C$ stands for the spreading sequence and subcarrier index. C is the number of spreading sequences. The $(g, (c-1)N_c + n)$ entry of $\mathbf{M}_C$ stands for the cth spreading sequence and its responding to nth subcarrier resource in the gth spatial group, and if this spreading sequence and subcarrier resource have been allocated to the users; the $(g, (c-1)N_c + n)$ entry of $\mathbf{M}_C$ denoted by $c_{g,c,n}$ is set to "0" (or otherwise "1").

The proposed method is to schedule the users to start from the group g_0 whose set S_{g_0} contains the largest number of users needed to be scheduled because such spatial group can provide the greater flexibility in user scheduling.

The index of such group is denoted by

$$g_0 = \arg\max_{g \in [1,G]} \left(N_{S_g}\right), \tag{11}$$

$$N_{S_g} = \sum_{u \in S_g,\, n \in [1, N_c]} m_{g,u,n}. \tag{12}$$

Based on the set of user indexes S_{g_0}, we can select the uth user who requests the resource of spatial group g_0 (i.e., $u \in S_{g_0}$) to form the set S_u, which contains the spatial group indexes requested by the uth user (i.e., $g \in S_u$). Then we can obtain $N_u^{\min}$ via

$$N_u^{\min} = \min_{g \in S_u} \left(N_{S_g}\right). \tag{13}$$

If uth user belongs to spatial group S_{g_0} and also fulfilling the condition

$$u = \arg\max_{u \in S_{g_0},\, g \in S_u} \left(N_u^{\min}\right), \tag{14}$$

then, we will allocate the spreading sequence and subcarrier resources of spatial group g_0 to the uth user. The above process follows the scheduling principle; that is, the scheduled user needs to satisfy the following:

(1) Its spatial groups have the largest number of users which need to be scheduled.

(2) After this user is scheduled, the maximal spatial and code resource can be left for the next loop to perform resource allocation.

Afterwards, the scheduled user, the allocated spreading sequence, and subcarriers need to be marked in the scheduling matrix $\mathbf{M}_S$ and resource matrix $\mathbf{M}_C$. Then repeat the above process until there are no resources to allocate.

To sum up, the proposed scheme can be described as follows:

(I) Partition users into predetermined G spatial groups based on their CSI.

(II) Select $1, \ldots, U$ users where SINR $> V_{\text{SINR}}$ from the users which need to be scheduled.

(III) Initialize sets S_g, S_u and matrixes $\mathbf{M}_S$, $\mathbf{M}_C$ based on step (I) and step (II).

(IV) Set $i = 0$.

(V) *While* $i \leqslant G * C * N_c$:

(a) increase i by 1,

(b) update S_u and S_g,

(c) select the set S_{g_0} based on (11),

(d) schedule the user u in group g_0 based on (13) and (14),

(e) allocate the resource indices (g, c, n) to user u,

(f) replace the element of gth row and $(u-1)N_c + n$ column with 0 in $\mathbf{M}_S$: that is, $m_{g,u,n} = 0$,

(g) replace the element of gth row and $(c-1)N_c + n$ column with "0" in $\mathbf{M}_C$: that is, $c_{g,c,n} = 0$,

(h) *if* $\mathbf{M}_C$ or $\mathbf{M}_S$ is a zero matrix, *break*.

(VI) *End while.*

In the above process, for each loop, one spreading sequence and subcarrier in one spatial group are allocated to a selected user. Therefore, the total number of loops is equal to the number of scheduled users of the system. According to the objective of the number of active users maximization, the scheduling method is considered to be optimum if the number of loops is maximized. However, in general, the proposed method cannot guarantee such global optimality. Instead, it can achieve local optimality by giving the maximal number of residual scheduling resources for the next loop to perform resource allocation.

In the case of existing multiple solutions to (11), we select a spatial group as S_{g_0} with its term $\max(N_u^{\min})$ to be the maximum among all the candidates. Based on our discussions above, such selection maintains the suboptimality of the proposed method.

3.4. Performance Analysis. As the spatial DOF is introduced as a critical factor to maximize the number of active users in the proposed scheduling scheme, the probability of attaining maximal DOF can be employed to analyze the scheme performance [24].

We define $\rho_{u,g,c,n}$ to be the probability for the uth user to be scheduled to the cth spreading sequence and nth subcarrier in the gth spatial groups and assume U users are distributed evenly onto G orthogonal spatial groups where there exist GCN_c unassigned spatial-code and frequency resources which are statistically independent with each other. Meanwhile, we assume $\rho_{u,g,c,n}$ $\forall u, g, c, n$, are identical with respect to the indexes (u, g, c, n), and thus $\rho_{u,g,c,n}$ is denoted by ρ.

For the first user, there exist GCN_c unassigned spatial-code resources in a subcarrier. Hence, the probability for the first user to have one spatial-code resource to access is

$$\sum_{g=1}^{G} \sum_{c=1}^{C} \sum_{n=1}^{N_c} \rho_{u,g,c,n} = GCN_c \rho. \tag{15}$$

Once the first user is assigned, the second user has only $GCN_c - 1$ options. Accordingly, the uth user has only $GCN_c - u + 1$ options, and its probability to have one resource to access is $(GCN_c - u + 1)\rho$.

Hence, the probability for all of GCN_c users to be assigned is

$$\prod_{u=1}^{GCN_c} \left(\left(GCN_c - u + 1 \right) \rho \right) = \left(GCN_c \right)! \rho^{GCN_c}. \tag{16}$$

In total, there exist $C_U^{GCN_c}$ groups as above; thus, the overall probability of achieving the maximal degree of freedom is given by

$$\text{Prob}_{\max} = \binom{U}{GCN_c} \left(GCN_c \right)! \rho^{GCN_c}. \tag{17}$$

From equation (17), it can be observed that the maximal spatial-code domain DOF can be attained with very high probability for the proposed scheme when the number of users U is large (e.g., massive number of IoT devices).

3.5. Computational Complexity Discussion. For the proposed scheme, the computational complexity mainly comes from the order statistics in (11)–(14). Given the maximal DOF of GCN_c, the complexity of order statistics in (11) is upper bounded by $O((UGN_c)^2)$; the same upper bound applies also to the procedure from (12) and (14). Since the maximal number of loops is GCN_c, the overall computational complexity is upper bounded by $O((UGN_c)^2 GCN_c)$, which is significantly lower than the exponential complexity offered by the brute-force search [25].

4. Performance Evaluation and Analysis

In this section, computer simulations were used to evaluate the proposed schemes in terms of the probability of attaining

Table 1: Major simulation parameters.

Parameters	Values
Tx power	23 dBm for 3D-UMa 500 m for UEs and IoT devices
Duplex	FDD
Tx antenna configurations	Tx antenna elements config.: 1 omni for both UEs and IoT devices
Rx antenna configurations	BS Rx antenna elements config: $8 \times 4 \times 2(\pm 45)$, $0.5\,\lambda$ H/$0.8\,\lambda$V
Traffic model	Date rate 0.5 Mbps TR36.814 Ftp model 2 for UEs [17] Data rate 80 kbps for IoT devices
Modulation	AMC for UEs QPSK for IoT devices
Coding scheme	AMC for UEs Turbo Code (code rate 0.23) for IoT
System bandwidth	10 MHz (50 PRBs)
Power control	Open loop fractional power control for UEs; alpha = 0.7 $P0 = -80$ dBm
Network synchronization	Synchronized
MUSA	Spreading sequences are generated by pseudorandom sequences
UE distribution	Number of UEs = 300, distribution according to 36.873 [18], Poisson arrival with rate 10/sec
IoT distribution	Number of devices varied from 1 to 30000 in steps of 3000, distribution according to 36.873 Access intensity as traffic model 2 in [19]
	Non-ideal channel estimation
Receiver	MMSE-IRC, detailed guidelines according to Rel-12 assumptions [20]
SRS	1Tx, 5 ms periodicity, wideband

maximal number of active users, the collision rate, and throughput performance.

In our simulation, there is a single BS (Macro) covering an area that includes UEs and IoT devices. BS is equipped with antenna array of 8×8 x-pol elements. For the simulation, there are $G = 8$ prebeamforming groups by using prebeamforming vectors $\mathbf{V}_g$, $g \in 1, \ldots, 8$ which can be given by the unitary DFT matrix $\mathbf{F}$ of size 8×8. $\mathbf{V}_g$ is formed by taking the $(g\text{-}1) \times r + 1$, $r = 1$. Hence, UEs and IoT devices in serving cell can be partitioned into eight spatial groups based on their CSI estimation. For IoT scheduling, the threshold of SINR V_{SINR} is 0 dB. The major simulation assumptions are listed in Table 1.

4.1. The Probability of Attaining Maximal Number of Active IoT Devices. Figure 3 displays the simulation results of the probability of obtaining maximal number of active users for the joint spatial-code scheduling scheme and the brute-force scheme. It can be observed that, with the number of IoT devices varying from 3000 to 30000, the probability of attaining maximal number of active users increases from about 50% to 90%. Meanwhile, the result shows that the probability of the proposed scheme and the brute-force scheme is almost the same to each other and the trend of simulation results is coincided with that of analytical method of (17).

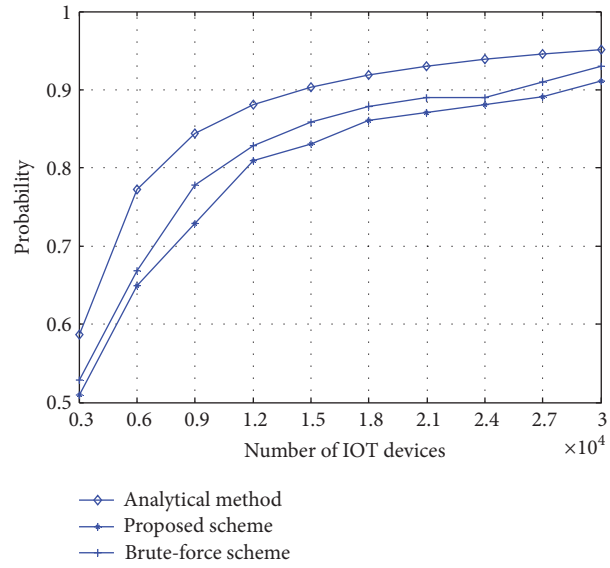

Figure 3: The probability of attaining maximal number versus the number of IoT devices.

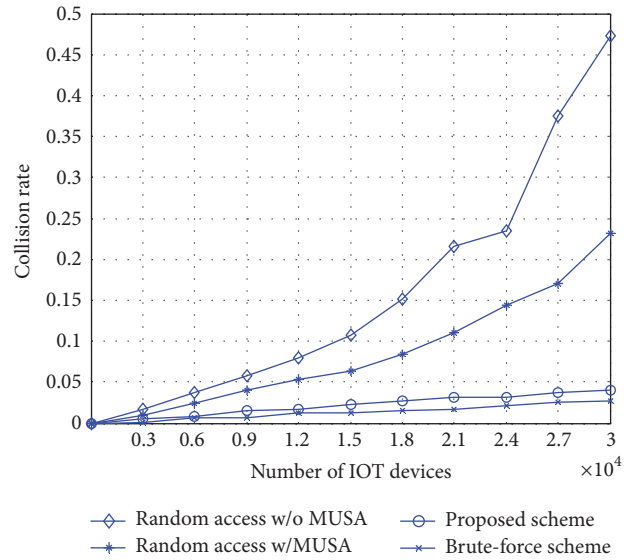

Figure 4: Collision rate versus the number of IoT devices.

4.2. The Collision Rate of Random Access. Let us denote total number of devices which send random access request as K_p and total number of devices that experienced collision as K_c. Then, we define the collision rate C_R as

$$C_R = \frac{K_C}{K_P}. \tag{18}$$

Figure 4 displays the collision rate of the preconfigured access scheme against the random access scheme with and without MUSA and the brute-force scheme with different numbers of IoT devices.

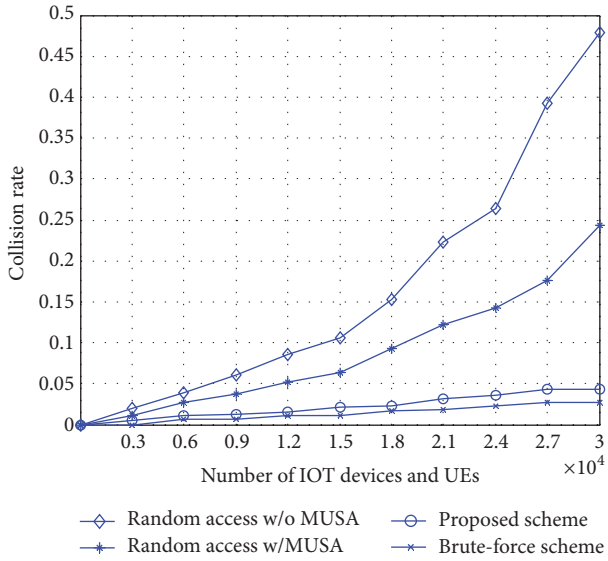

Figure 5: Collision rate versus the number of IoT devices and UEs.

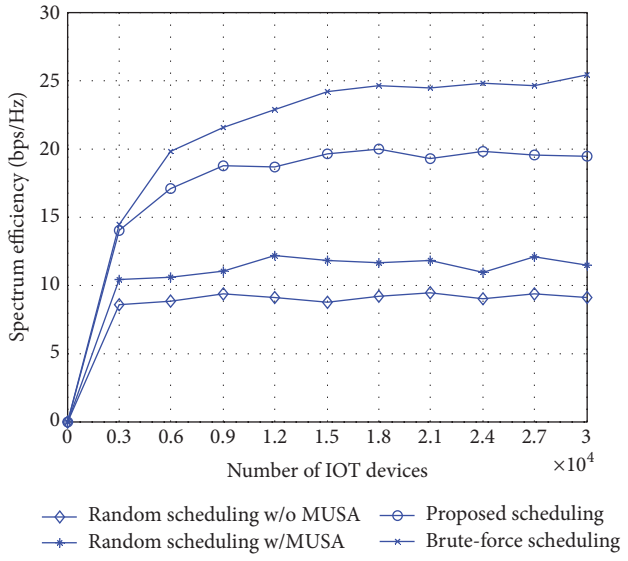

Figure 6: Cell average spectrum efficiency (SE) comparison versus the number of IoT devices.

The results show that, with the number of IoT devices from 3000 to 30000, the collision rates of the random access scheme without MUSA increase from 1.7% to 47.2% and the collision rates of the random scheme with MUSA increase from 0.9% to 23.2%. As introduced in the spatial DOF, the collision rate of the proposed scheme can reduce to about 5% when the number of IoT devices is 30000. From Figure 4, it can also seem that the performance of the proposed scheme and the brute-force scheme is close to each other.

Figure 5 displays the performance of these schemes with different numbers of IoT devices and UEs. The results show that the proposed access scheme still has the better performance than the random access scheme. Meanwhile, as the number of UEs is very small compared with IoT devices, they have no effect on the result of collision rate. Hence, the simulation results of collision rate with UE and IoT random access in Figure 5 are almost the same to the results of only IoT random access in Figure 4.

4.3. Throughput Performance. The simulation results of cell average spectrum efficiency are provided in Figures 6 and 7. Figure 6 displays the cell spectrum efficiency of the proposed scheme, the random scheduling scheme with and without MUSA and the brute-force scheme versus the number of IoT devices. The results show that the proposed scheme can achieve higher average spectrum efficiency than the random scheduling both with and without MUSA as it can achieve additional spatial-domain multiplexing gain. The proposed scheme achieves about 63.3% and 104.9% of the mean improvement rate of spectrum efficiency compared with the random scheduling with and without MUSA, respectively, with the number of IoT devices varying from 3000 to 30000 per cell.

Figure 7 displays the average spectrum efficiency of these schemes versus the number of IoT devices and UEs. It can be observed that the proposed scheme still have the

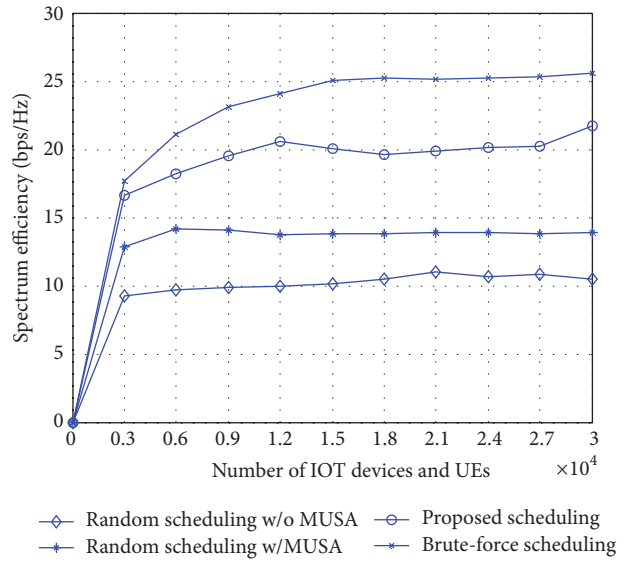

Figure 7: Cell average spectrum efficiency (SE) comparison versus the number of IoT devices and UEs.

significant performance gain compared with the random scheduling scheme with and without MUSA and the mean improvement rate of spectrum efficiency is about 42.4% and 91.9%, respectively. Furthermore, as AMC is used in uplink UE scheduling procedures, the data transmission of UEs can achieve higher spectrum efficiency than IoT devices in the hybrid scheduling of UEs and IoT devices. Therefore, the results of spectrum efficiency in Figure 7 are higher than that in Figure 6.

From Figures 6 and 7, it can be observed that the proposed scheduling scheme has the similar performance to the brute-force scheme with computation complexity reduction.

5. Conclusion

In this paper, two novel schemes are proposed to enhance random access and improve the system capacity for IoT communication based on user spatial grouping.

In the proposed preconfigured access scheme, the preamble resources are multiplexed to reduce the collision rate of random access based on user spatial grouping. In the proposed joint scheduling scheme, each IoT device is identified with a set of spatial-code indices; based on these indices, BS can schedule users to transmission on the same time-frequency resources to achieve additional spatial-domain multiplexing gain. The simulation results validate that the preconfigured access scheme can obviously reduce the collision rate and the proposed scheduling scheme can achieve about 63.3% and 104.9% of the mean improvement rate of spectrum efficiency compared with the random scheduling with and without MUSA, respectively. Furthermore, the results show that the proposed scheduling scheme can achieve similar performance to brute-force scheme with lower scheduling complexity.

Disclosure

Qi Bi is a Fellow at IEEE. Bin Han is currently working at China Telecom Corporation Limited Technology Innovation Center.

Competing Interests

The authors declare that there is no conflict of interests regarding the publication of this article.

References

[1] L. Atzori, A. Iera, and G. Morabito, "The internet of things: a survey," *Computer Networks*, vol. 54, no. 15, pp. 2787–2805, 2010.

[2] 3GPP R1-142919, "Narrow band LTE for MTC in LTE Rel-13," MediaTek, RAN1#78, August 2014.

[3] J. Gozalvez, "New 3GPP Standard for IoT," *IEEE Vehicular Technology Magazine*, vol. 11, no. 1, pp. 14–20, 2016.

[4] F. Boccardi, R. Heath Jr., A. Lozano, T. L. Marzetta, and P. Popovski, "Five disruptive technology directions for 5G," *IEEE Communications Magazine*, vol. 52, no. 2, pp. 74–80, 2014.

[5] A. Osseiran, F. Boccardi, V. Braun et al., "Scenarios for 5G mobile and wireless communications: the vision of the METIS project," *IEEE Communications Magazine*, vol. 52, no. 5, pp. 26–35, 2014.

[6] M. Kasparick, G. Wunder, P. Jung, and D. Maryopi, "Bi-orthogonal waveforms for 5G random access with short message support," in *Proceedings of the 20th European Wireless Conference (EW '14)*, pp. 293–298, Barcelona, Spain, May 2014.

[7] Y. Saito, Y. Kishiyama, A. Benjebbour, T. Nakamura, A. Li, and K. Higuchi, "Non-orthogonal multiple access (NOMA) for cellular future radio access," in *Proceedings of the IEEE 77th Vehicular Technology Conference (VTC '13)*, pp. 1–5, Dresden, Germany, June 2013.

[8] J. Van De Beek and B. M. Popović, "Multiple access with low-density signatures," in *Proceedings of the IEEE Global Telecommunications Conference (GLOBECOM '09)*, pp. 1–6, December 2009.

[9] M. Al-Imari, P. Xiao, M. A. Imran, and R. Tafazolli, "Uplink non-orthogonal multiple access for 5G wireless networks," in *Proceedings of the 11th International Symposium on Wireless Communications Systems (ISWCS '14)*, pp. 781–785, August 2014.

[10] H. Nikopour and H. Baligh, "Sparse code multiple access," in *Proceedings of the IEEE 24th Annual International Symposium on Personal, Indoor, and Mobile Radio Communications (PIMRC '13)*, pp. 332–336, IEEE, London, UK, September 2013.

[11] L. Dai, B. Wang, Y. Yuan, S. Han, C. I, and Z. Wang, "Non-orthogonal multiple access for 5G: solutions, challenges, opportunities, and future research trends," *IEEE Communications Magazine*, vol. 53, no. 9, pp. 74–81, 2015.

[12] P. K. Wali and D. Das, "A novel access scheme for IoT communications in LTE-Advanced network," in *Proceedings of the IEEE International Conference on Advanced Networks and Telecommunication Systems (ANTS '14)*, pp. 1–6, New Delhi, India, December 2014.

[13] E. G. Larsson, O. Edfors, F. Tufvesson, and T. L. Marzetta, "Massive MIMO for next generation wireless systems," *IEEE Communications Magazine*, vol. 52, no. 2, pp. 186–195, 2014.

[14] K. Zheng, L. Zhao, J. Mei, B. Shao, W. Xiang, and L. Hanzo, "Survey of large-scale MIMO systems," *IEEE Communications Surveys & Tutorials*, vol. 17, no. 3, pp. 1738–1760, 2015.

[15] T. L. Marzetta, "Noncooperative cellular wireless with unlimited numbers of base station antennas," *IEEE Transactions on Wireless Communications*, vol. 9, no. 11, pp. 3590–3600, 2010.

[16] Z. Jiang, B. Han, P. Chen, F. Yang, and Q. Bi, "Design of joint spatial and power domain multiplexing scheme for massive MIMO systems," *International Journal of Antennas and Propagation*, vol. 2015, Article ID 368463, 10 pages, 2015.

[17] 3GPP TR36.814 V9.0.0, "Further advancements for E-UTRA physical layer aspects," March 2010.

[18] 3GPP TR36.873 (V12.2.0), "Study on 3D channel model for LTE," July 2015.

[19] 3GPP TR 37.868 V0.8.1, 'Study on RAN Improvements for Machine-type Communications', August 2011.

[20] 3GPP TR36.866 (V12.0.1), "Study on network-assisted interference cancellation and suppression (NAIC) for LTE," March 2014.

[21] B. Wang, K. Wang, Z. Lu, T. Xie, and J. Quan, "Comparison study of non-orthogonal multiple access schemes for 5G," in *Proceedings of the 10th IEEE International Symposium on Broadband Multimedia Systems and Broadcasting (BMSB '15)*, Ghent, Belgium, June 2015.

[22] L. Dai, Z. Wang, and S. Chen, "A novel uplink multiple access scheme based on TDS-FDMA," *IEEE Transactions on Wireless Communications*, vol. 10, no. 3, pp. 757–761, 2011.

[23] J. Nam, A. Adhikary, J.-Y. Ahn, and G. Caire, "Joint spatial division and multiplexing: opportunistic beamforming, user grouping and simplified downlink scheduling," *IEEE Journal on Selected Topics in Signal Processing*, vol. 8, no. 5, pp. 876–890, 2014.

[24] J. Hou, N. Yi, and Y. Ma, "Joint space-frequency user scheduling for MIMO random beamforming with limited feedback," *IEEE Transactions on Communications*, vol. 63, no. 6, pp. 2224–2236, 2015.

[25] A. Levitin, *Introduction to the Design & Analysis of Algorithms*, Pearson Educ, Harlow, UK, 3rd edition, 2011.